

Radiation Hard Strip Detectors on Oxygenated Silicon

L. Andricek, G. Lutz, H.G. Moser, R. H. Richter

Abstract—Recent results of the RD48 (ROSE) collaboration suggest the usage of oxygen enriched silicon for sensors operated in the harsh radiation environment of future high luminosity experiments. To investigate if the anticipated beneficial properties are still present after full processing of the wafers, strip detectors for the innermost ring of the ATLAS forward region have been fabricated on oxygen enriched silicon by CiS, Germany. These sensors, together with sensors on standard and thin substrates, have been exposed to $3 \cdot 10^{14}$ 24 GeV/c protons/cm² at the CERN PS. We are presenting here the comparison between the sensors based on the CV measurements and the investigation of the charge collection efficiency obtained with a ⁹⁰Sr source and the analogue readout chip SCT128A.

Keywords—Silicon Detectors; Radiation Hardness; Silicon Oxygenation

I. INTRODUCTION

Exposing detectors to the radiation environment at LHC will induce bulk defects with concentrations exceeding by far those of the original dopants. The well known consequences of the bulk material changes are an increase of detector leakage current, the change of effective doping from n- to p-type (type inversion) followed by a steady increase of full depletion voltage, and signal loss due to enhanced charge trapping after radiation damage. A careful design of the sensors can cope with these changes in the basic properties of the bulk silicon and allow operating voltages up to several hundred volts[1]. The RD48 (ROSE) Collaboration is concentrating it's work on the hadron induced change in the silicon bulk. Their results, mainly obtained through irradiation and characterisation of simple test diodes, lead to the insight, that a higher oxygen enrichment of the silicon bulk is advantageous for several reasons[2]. Firstly, if the radiation environment contains a significant component of charged hadrons, the effective doping concentration after irradiation is lowered by oxygenation of the material. Secondly, the reverse annealing saturates at fluences above $2 \cdot 10^{14}$ p/cm² and the rate of growth of the effective doping density with time after irradiation is a factor 2 to 4 slower at the same temperature. As a consequence the sensors can be kept for a longer period at room temperature, which gives an additional safety margin, if longer maintenance periods are needed in the experiment. As a final step these two approaches, the careful design and the oxygen enrichment, have to be combined and the full technology has to be implemented in the process of a company, capable of the large scale production for the future LHC experiments. Therefore the design and technology of the MPI Semiconductor Laboratory (Halbleiterlabor) have been transferred

to CiS, Germany, who did the oxygen enrichment in their process furnances and the fabrication of the sensors on this material.

A second approach to have a full depleted p⁺n detector after type inversion at moderate voltages is the usage of a thinner bulk. One intention of this paper is therefore the direct comparison between standard, thin standard, and oxygenated full size strip detectors which have undergone exactly the same processing steps, irradiated up to the same fluence, and read out with electronics at LHC speed.

II. DETECTOR DESIGN AND PRE-IRRADIATION CHARACTERISTICS

The basic design features, including the edge region and the properties of the p⁺n detectors after type inversion, are described already in [1]. The detectors tested here are wedge shaped, designed for the innermost ring of the ATLAS forward region[4]. They have 768 capacitively coupled readout strips with an active length of 7.2 cm, biased via implanted resistors. The mean pitch is 61.7 μm and the active surface of the detectors is ≈ 35 cm².

Most of the tested sensors have been processed on oxygen enriched high resistivity material (2 to 5 kΩcm, <111>, nominal thickness 285 μm). The oxygen diffusion was performed by placing oxidized wafers into a process furnace at 1150°C in an inert ambient (N₂) for 3×8 h [5]. After this process the oxygen concentration in the middle of the wafers, measured on a separate wafer by the SIMS method, was $\approx 10^{17}$ at/cm³, the carbon concentration was $\approx 7 \cdot 10^{15}$ at/cm³[6]. To allow a direct comparison, one de-

TABLE I

Summary of the tested detectors with their thicknesses and the currents before irradiation, mounted and bonded, at room temperature

| Detector | t[μm] | O ₂ ? | I@150V[μA] | I@350V[μA] |
|----------|---------------|------------------|------------|------------|
| 3688-01 | 246 | no | 1.5 | 2.0 |
| 3689-03 | 260 | no | 3.8 | 4.6 |
| 3688-19 | 274 | no | 1.0 | 1.2 |
| 3688-21 | 285 | 3×8h | 4.4 | 15.0 |
| 3689-22 | 279 | 3×8h | 1.0 | 1.4 |
| 3688-20 | ≈ 285 | 3×8h | 1.3 | 1.5 |
| 3688-22 | ≈ 285 | 3×8h | 0.9 | 1.5 |
| 3688-24 | ≈ 285 | 3×8h | 0.8 | 1.6 |
| 3689-23 | ≈ 285 | 3×8h | 1.3 | 1.7 |

detector on standard 285 μm thick material and two "thin" detectors on 260 μm standard material with the identical layout have been in the same irradiation. The oxygen, resp. carbon concentration in the middle of the standard wafers is $\approx 7 \cdot 10^{15}$ at/cm³, resp. $\approx 2 \cdot 10^{15}$ at/cm³[6]. All the detectors have been glued to support ceramics and all strips have been bonded via a glass pitch adaptor to a common rail, connected to electrical ground. The currents have been measured after this mounting procedure and the results are shown in the summary Table 1. The currents of all the detectors are very similar, except 3688-21, which shows a higher current. This higher current is most likely due to the mounting and bonding procedure. It can be stated that there is no systematic difference in the currents of detectors on oxygen enriched and standard material before irradiation.

III. DETECTOR CHARACTERISTICS AFTER IRRADIATION

The irradiation of the nine detectors was carried out in two steps at the CERN PS. The first irradiation (Nov.'99) was done with three detectors fabricated on standard silicon and two on oxygen enriched material. Two of the standard material detectors were approximately 30 μm thinner to reduce the full depletion voltage after irradiation by roughly 20%. The last four oxygen enriched detectors from Table 1 were irradiated during another period (June'00) in the same setup. In both cases the detectors were biased at 100 V and cooled at $\approx -10^\circ\text{C}$ during irradiation. Currents were monitored and recorded throughout the entire irradiation. A typical evolution of the currents with fluence is seen in Fig. 1. The two curves are the currents of a standard (lower current at fluences higher than $1 \cdot 10^{14}$ p/cm²) and an oxygen enriched detector (higher current at high fluences) at 100 V. At this bias voltage the detectors go from full depletion (which is at ca. 75 V before irradiation) through type inversion to partial depletion with increasing fluence. Following a simple model from [7] and neglecting the small effect of annealing at low temperatures, the current in the low fluence region is expected to increase linearly with the fluence. Beyond type inversion the effective doping increases with fluence and the depleted volume shrinks, if the bias voltage is kept constant. Using the parametrization

$$\Delta I = \alpha \cdot \phi \cdot Vol \quad (1)$$

and

$$N_{eff}(\phi) = N_{eff}(0) \cdot e^{-c\phi} - \beta \cdot \phi \quad (2)$$

for the change in the volume generated current and the effective doping concentration due to irradiation, a linear fit to the low fluence data gives the damage parameter α . The first term in equation 2 describes the exponential donor removal at lower fluences and the second the acceptor creation part with the linear increase of the effective doping concentration for higher fluences[8]. For high fluences the current is a function of the width of the space charge region and therefore the effective doping concentration. Using the

equation for the width of the depleted region

$$w = \sqrt{\frac{2\epsilon V_{bias}}{e |N_{eff}|}} \quad (3)$$

leads to the expected current at high fluences

$$I = \alpha A \sqrt{\frac{2\epsilon V_{bias}}{e \beta}} \sqrt{\phi} \quad (4)$$

which gives the parameter β for the acceptor creation. In this equations A is the area of the detector, Vol the volume of the depleted region, ϵ the dielectric constant of silicon, e the electron charge, and V_{bias} the applied bias voltage. In addition to this bulk generated current there is an edge generated current due to the fact that the silicon is now inverted and the space charge region extends from the n⁺ backside touching the highly damaged cut region[9]. The fits are shown in Fig. 1 for both, the standard and oxygen enriched detector. The results for the damage parameters (α is scaled to 20°C) are listed in Table 2. It's clearly visible that already at this stage of irradiation and negligible annealing the current characteristics of the two materials are almost identical, but the change in the effective doping concentration is about 30% lower for the oxygen enriched material.

TABLE II

Damage parameters extracted from the currents during irradiation (24 GeV/c protons).

| Detector | α at 20°C [A/cm] | β [1/cm] |
|------------|-------------------------|----------------|
| standard | 4.04e-17 | 0.063 |
| oxygenated | 3.96e-17 | 0.044 |

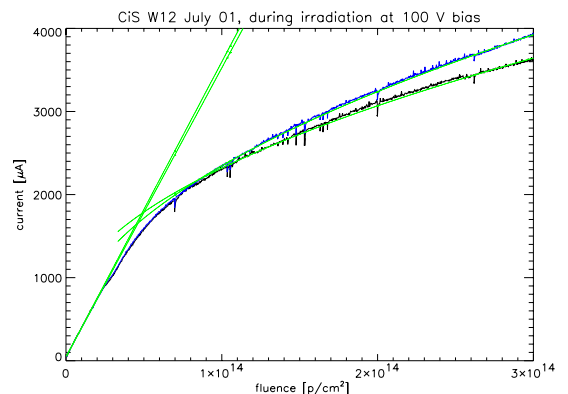


Fig. 1. Currents of two detectors during irradiation normalized to 20°C together with the fit results. The lower curve is the standard detector, the upper curve the oxygen enriched one (see text).

After irradiation the detectors went through a standardized annealing procedure for 7 days at 25°C in order to reach the flat minimum of the full depletion voltage at the end of the beneficial annealing. The current voltage char-

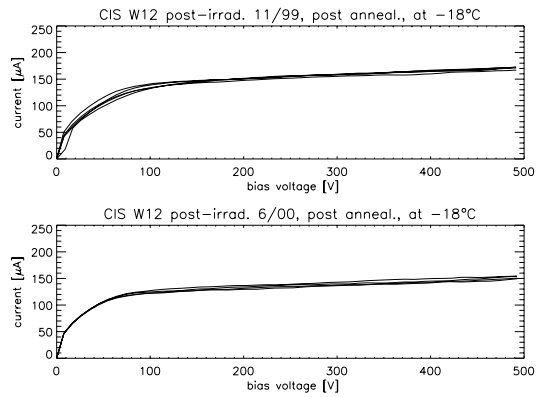


Fig. 2. IV curves one detector on standard, two on standard thin and two on oxygen enriched material (upper plot), and of four detectors, all on oxygen enriched material (lower plot), after two different irradiations to the same nominal fluence and 7 days annealing at 25°C.

acteristics of the 9 detectors after irradiation and first annealing are shown in Fig. 2. The currents were measured at -18°C inside of a temperature controlled cabinet. The upper plot in Fig. 2 shows the results of the first irradiation of the detectors with various thicknesses. The currents at 350 V of all the detectors are around $165\ \mu\text{A}$ with almost no dependency on the thickness. This becomes somewhat clearer, if one looks at the currents in the lower plot of Fig. 2, where four identical oxygen enriched detectors with the same nominal thickness have been measured and where the variation in the individual currents is similar. Even for this identical detectors the variation of the individual currents is in the order of 10%. The absolute value of the currents at 350 V and -18°C is here around $145\ \mu\text{A}$. The reasons for the difference between these two irradiation results are mainly due to the uncertainty in the fluence during the irradiation (which is estimated to be at the level of 10%) and the uncertainty in the actual temperature inside the cabinet where the measurements were performed. Within these errors, there is no difference between the currents of detectors on oxygen enriched and standard material.

A. Static Measurements after Irradiation, Long Term Annealing

To investigate the differences between the various detector materials, the first five detectors from Table 1 have been taken through an annealing procedure far beyond the point of the minimal depletion voltage. In order to reduce the time requirements the annealing was performed at 30°C . This was then scaled to 25°C using the parametrisation from [10]. The procedure went on until an equivalent annealing time of 32 days at 25°C was reached. Throughout this annealing period, every few days the detectors were cooled down to -18°C to do the IV and CV measurements at different annealing stages. The CV measurements were done at a frequency of 100 Hz (the lowest possible with the LCR meter used). The "full depletion" voltage from this CV curves was extracted by a simple fit. It represents the voltage where the curve of $1/C^2(V)$ goes into saturation.

The IV curve was measured simultaneously. Fig. 3 shows the evolution of the currents (normalized to 20°C) at 350 V with annealing time and the damage parameter α 24 GeV/c protons extracted from this measurements. It starts at $4.0 \cdot 10^{-17}\ \text{A/cm}$ shortly after irradiation and reaches for long annealing times $2.0 \cdot 10^{-17}\ \text{A/cm}$. It was found to be the same for all detectors independent of the oxygen concentration in the substrate. The advantage of oxygen

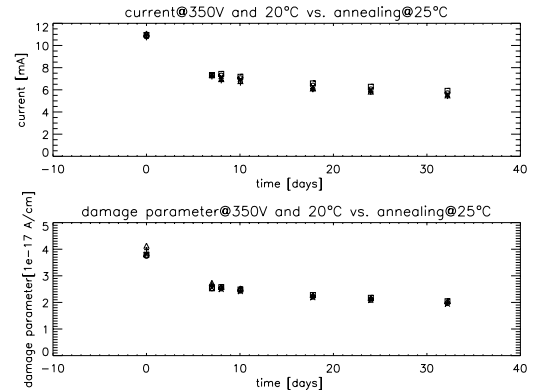


Fig. 3. Annealing of the current and the damage parameter α for 24 GeV/c protons.

enriched detector material becomes evident, if one looks at the "full depletion voltage" extracted from CV measurements. This is shown in Fig. 4. The difference in the full depletion voltage between standard and oxygen enriched material is minimal at the end of the beneficial annealing and increases with annealing time. The lower plot in Fig. 4, where the full depletion voltages from the CV curves are normalized to $300\ \mu\text{m}$ thickness, makes the difference between the two materials used even more distinct and shows clearly the suppression of the reverse annealing for oxygen enriched material. Table 3 summarises these results.

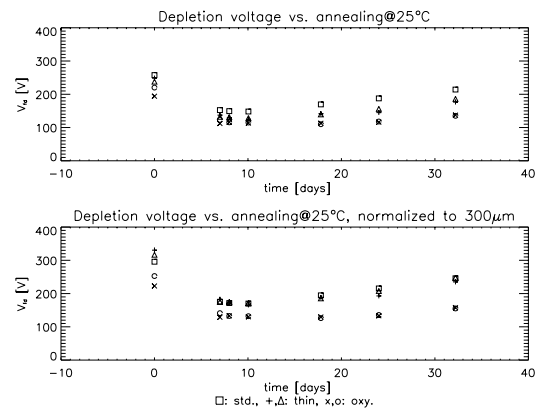


Fig. 4. Development of the full depletion voltage with annealing time.

B. Charge Collection Efficiency

The differences between the full depletion voltages from CV curves of the standard and the oxygenated material of

TABLE III

Full depletion voltages from CV curves for the various detector types.

| Detector | V_{fd} After 7d at 25°C | V_{fd} After 32d at 25°C | reverse annealing |
|------------|------------------------------|-------------------------------|----------------------|
| standard | 149 V | 214 V | 65 V |
| thin | 130 V | 181 V | 51 V |
| oxygenated | 115 V | 136 V | 21 V |

the same thickness are 34 V after 7 days and 78 V after 32 days at 25°C. To investigate whether these differences can be seen also in the charge collection efficiency, 128 channels of the detectors were bonded to a single SCT128A chip [11]. The frontend of this chip has a risetime of approx. 20 ns and the input stage is identical to that of the ABCD chip [12], the binary chip to be used in ATLAS SCT. But unlike the binary chip it has the advantage that the analogue information for each channel is directly accessible event by event. Thus making it fairly easy to extract reliable information on detector performance before and after irradiation.

Signal measurements were performed with a ^{90}Sr beta source. Signals from up to five consecutive strips are included in a signal cluster, assumed to include all signal charge generated by a traversing electron. Such a cluster is initiated by a seed of a strip with 4σ signal and accepted when it has a total charge of at least 5σ above the average noise of the particular channels. A Landau distribution (convoluted with a Gaussian) is fitted to the obtained pulse height spectrum.

The first measurements on 2 oxygenated, 2 thin and one standard material detector have been done after 7 days annealing. The signal heights were then normalized to the signals from an unirradiated detector of 285 μm nominal thickness. All the measurements (also with the unirradiated detector) have been done at approx. -20°C and with the readout in exactly the same operating conditions. The result is shown in Fig. 5. The onset of the plateau for the full CCE is extracted by a simple fit of two straight lines as shown in Fig. 5, in order to get comparable numbers for the three substrate types. This onset of the plateau is about 60 V lower for the oxygenated detectors. The situation for the thin detectors on standard material is less clear as this voltage depends of course on the actual thickness of the detector. The thinner detector (246 μm) shows about the same onset voltage as the oxygenated ones, but the penalty for this is a smaller signal.

These measurements have been repeated after the long term annealing. Fig. 6 shows the comparison between the standard and the oxygen enriched detector after 32 days at 25°C. The effect of reverse annealing of the standard detector is here much smaller than expected from the CV measurements. The voltage at the onset of the plateau increases only by 36 V for the standard detector and 32 V for the oxygenated one. The expected values from the CV

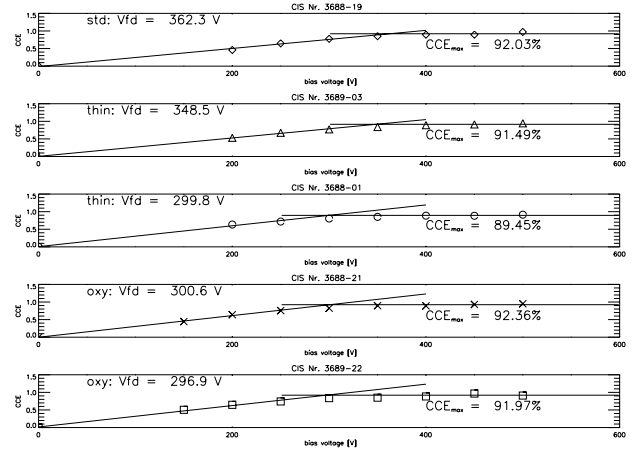


Fig. 5. Charge Collection Efficiencies (normalized to signals from an unirradiated detector of the same batch) for the standard, thin, and oxygen enriched detectors after 7 days annealing at 25°C.

measurements are 65 V for standard, resp. 21 V for oxygen enriched material. The reason for this is in the way the data is analysed. In the way described above we are summing up up to five consecutive strips to get the cluster charge. Due to the intrinsic nature of undepleted irradiated silicon[13], the generated charge induces a signal in the readout strips even in under-depleted mode. And secondly, it diffuses through the undepleted region and is collected by a number of strips instead of being focussed by an electric field on one or two single strips. This means that almost the full signal charge is detected even in under-depleted operation of the detector. Fig. 7 shows the fraction of the total charge in the highest hit. The small difference in the absolute value between the two detectors is most likely due to the fact that the position of the source relative to the detector and the scintillator for the trigger is not very well reproducible. A slight displacement leads to more inclined tracks and therefore to a bigger charge spreading over the readout strips. The interesting feature is the dependence of the fraction with bias voltage. It indicates that the charge spreading below 400 V is much bigger for the standard material than for the oxygenated one. In order to simulate

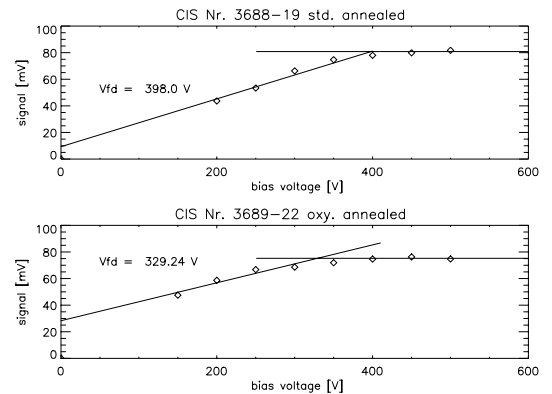


Fig. 6. Signal versus bias voltage for the detectors on standard and oxygenated material after 32 days annealing at 25°C.

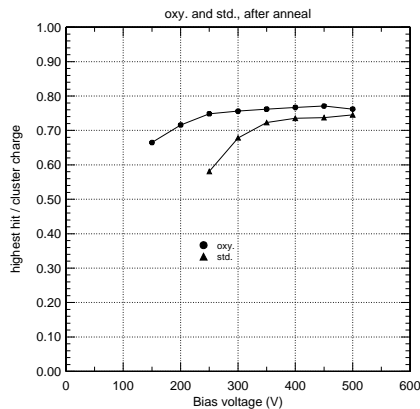


Fig. 7. Fraction of the charge in the highest hit versus the bias voltage after long term annealing

the binary front end electronics in ATLAS, where clustering will not be possible, the analysis of the data has been repeated taking only the highest hit within a cluster into account. The results are shown in Fig. 8. Compared to Fig. 6, the signal height at saturation is now about 25% lower due to the fact that in this way not all the charge is detected. The difference in the onset of the full CCE between standard and oxygen enriched material is now about 100 V, with the same S/N in the plateau.

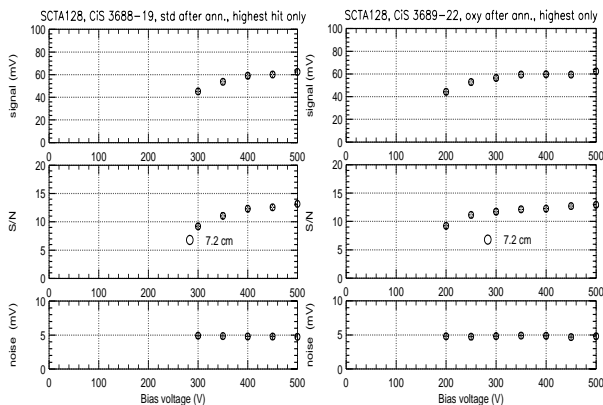


Fig. 8. Signal and S/N for the standard and oxygen enriched detector, looking only at the highest hit in a cluster.

IV. SUMMARY AND CONCLUSIONS

Six strip detectors on oxygen enriched material and three detectors on standard material, two of those on nominally $260\mu\text{m}$ thick material, have been irradiated up to a fluence of $3 \cdot 10^{14}$ 24 GeV p/cm^2 . The oxygen enrichment proposed by the ROSE collaboration has been integrated in the process line of a company capable of the large scale production needed for future LHC Experiments. The oxygen enrichment did not affect the IV characteristics of the detectors, neither before nor after the irradiation. After irradiation the detectors went through a controlled annealing procedure up to an equivalent annealing time of 32 days at 25°C . The difference in the effective doping concentration after irradiation has been investigated by CV and signal

measurements with a ^{90}Sr source and fast electronics. At the end of the 32 days annealing period, the difference in the full depletion voltage from CV measurements between standard and oxygen enriched material was found to be about 80 V lower for the oxygenated material. The difference obtained with measurements of the CCE with fast electronics (SCT128a) is about 100 V, if one looks only at the strip with the highest signal, simulating the use of binary electronics.

It was shown to be possible to build strip detectors on oxygen enriched material without deteriorating the basic characteristics of the devices before irradiation. After irradiation the lower effective doping concentration of oxygen enriched silicon leads to lower operating voltage giving an additional safety margin for safe operation in harsh radiation environments like in ATLAS.

V. ACKNOWLEDGMENTS

The authors would like to acknowledge the ATLAS group of the University of Sheffield, namely C.M. Buttar, I. Dawson, C. Grigson and R. Nicholson for setting up and maintaining the irradiation setup and monitoring system at the T7 beamline of the CERN PS. We also would like to thank M. Glaser and his colleagues for the reliable dosimetry and of course D. Joos from the University Freiburg and S. Kemmer from the MPI Halbleiterlabor for assembling and bonding the detectors.

REFERENCES

- [1] G. Lutz et al: "Radiation Hard Single Sided p^+n Detectors Optimized for Single Threshold Binary Readout"; 3rd International Symposium on Development and Application of Semiconductor Tracking Detectors, Melbourne Dez.1997
- [2] RD48 3rd Status Report, CERN/LHCC 2000-009, December 1999
- [3] L. Andricek et al.: "Single sided p^+n and double sided silicon strip detectors exposed to fluences up to $2 \times 10^{14}/\text{cm}^2$ 24 GeV protons."; presented at the 7th Pisa meeting on advanced detectors, La Biodola, Isola d'Elba, May 25-31, 1997; Nucl. Instr. and Meth. A 409 (1998) 184-193
- [4] ATLAS Inner Detector Technical Design Report, 1997
- [5] G. Casse et al: "Introduction of high oxygen concentrations into silicon wafers by high temperature diffusion", ROSE/TN/99-1 Technical Report. CERN, Geneva, 1999
- [6] Michael Moll, private communication
- [7] R.S. Harper et al.: "Evolution of silicon microstrip detector currents during proton irradiation at the CERN PS"; Nucl. Instr. and Meth. A, accepted for publication, April, 2001
- [8] G. Lindstrom et al.: "Radiation Hardness of silicon detectors - a challenge from high-energy physics"; Nucl. Instr. and Meth. A 426 (1999), 1-15
- [9] G. Lutz: "Survival of single sided n-bulk detectors after type inversion"; 2nd Workshop on radiation hardening of silicon detectors, CERN 4.-5. February 1997
- [10] H.J. Ziocck et al.: "Temperature Dependence of the Radiation Induced Change of Depletion Voltage in Silicon pin Detectors"; Nucl. Instr. and Meth. A 342 (1994) 96-104
- [11] E. Chesi et al.: "Performance of a128-channel analogue front-end chip for readout of Si strip detector modules for LHC experiments"; IEEE, Trans. on Nucl. Sci. Vol 47. no 4 (2000). 1434.
- [12] W. Dabrowski et al.: "Progress in Development of the Readout Chip for the ATLAS Semiconductor Tracker"; Proc. of the Sixth Workshop on Electronics for LHC Experiments, Krakow, 11-15 September 2000. CERN/LHCC/2000-41, 25 October 2000, p.115.
- [13] G. Lutz: "Effects of deep level defects in semiconductor detectors"; Nucl. Instr. and Meth. A 377 (1996) 234-243